International Journal of Mechanical Sciences 144 (2018) 531-539

Ultimate swelling described by limiting chain extensibility of swollen elastomers

Dai Okumura [*, 1] and *Shawn A. Chester* [2]

[1] Department of Mechanical Systems Engineering, Nagoya University,
Furo-cho, Chikusa-ku, Nagoya 464-8603, Japan

[2] Department of Mechanical Engineering, New Jersey Institute of Technology,
Newark, NJ 07102, USA

[*] Corresponding author.
E-mail address: dai.okumura@mae.nagoya-u.ac.jp (D. Okumura)

Abstract

In this study, we study ultimate swelling characterized by limiting chain extensibility of swollen elastomers. Limiting chain extensibility is introduced into the Flory–Rehner theory using the Arruda–Boyce eight chain model and the Gent phenomenological model. The difference between these models is unified by defining a single scalar function. The inequality derived from this function allows for analysis to provide an ultimate value of swelling ratio. This ultimate value is not exceeded at equilibrium swelling regardless of the set of material constants. Under uniaxial loading at equilibrium swelling, deswelling can occur even in tension. Further, the very large swelling behavior of pH sensitive hydrogels is found to originate from the resistance generated by approaching the ultimate value of swelling ratio.

Keywords: Elastomers, Swelling, Hyperelasticity, Limiting chain extensibility, Gels

1. Introduction

Swelling of elastomers by solvents was first investigated for the combination of natural rubbers and organic liquids [1,2]. Recently, a number of polymeric gels represented by hydrogels are regarded as swollen elastomers [3,4]. The Flory–Rehner theory is used to describe the mechanical and swelling behavior of swollen elastomers [1,5]. The free energy function consists of the sum of two terms associated with polymer stretching and the mixing of polymer and solvent molecules, which are derived from the Gaussian network theory (i.e., a Neo–Hookean (NH) model) and the Flory–Huggins solution theory, respectively. The Flory–Rehner theory has been systematically implemented into the commercially available finite element software [6,7], thereby allowing researchers to analyze a variety of swelling-induced mechanical problems [4,6,8,9]. However, the NH model may be too simple to describe the nonlinear elasticity of elastomers undergoing large deformations.

When the NH model in the Flory–Rehner theory is replaced by a more sophisticated strain-energy function for rubber elasticity, it is natural to consider models that include the non-Gaussian chain effect, i.e., the effect of limiting chain extensibility. In non-Gaussian network theory [2,10], the limited extensibility of the single chain is expressed approximately using the inverse Langevin function with an additional material constant, n, i.e., the number of rigid links in the single chain. Arruda and Boyce [11] developed the 8-chain model (AB model), which is based on a cubic representative cell containing 8 chains along diagonal directions (cf. 3- and 4-chain models). In contrast, the well-known phenomenological model by Gent [12] (G model) is a simple and accurate approximation of the AB model without the inverse Langevin function [13,14]. The G model has the additional material constant, J_m, instead of n used in the AB model. The AB and G models are appropriate to investigate the effect of limiting chain extensibility because the physical significance of the additional material constants, n and J_m, is clear.

Chester and Anand [15,16] and Li et al. [17] introduced the AB and G models to the Flory–Rehner theory, respectively, to investigate the effect of limiting chain

extensibility. Chester and Anand [15,16] compared the transient swelling response of a constrained gel predicted by Gaussian and non-Gaussian network theories. Here, the constant related with n was fixed and was not parameterized. Li et al. [17] showed that by adjusting J_m in the G model, the discrepancy of osmotic pressure functions was removed for very large swelling ratios of two different pH sensitive hydrogels. In addition, although Boyce and Arruda [18] investigated the use of the AB model, the effect of the swelling ratio on the stress–stretch behavior under uniaxial tension and compression did not involve the use of the Flory–Rehner theory; i.e., the swelling ratio was fixed during uniaxial loading. Thus, the effect of limiting chain extensibility on the mechanical responses of swollen elastomers is not sufficiently clear at full length.

In addition to those models described above based on the Flory–Rehner approach, other modeling approaches may be found in the literature. One such approach is based on the classical work of Terzaghi [19] and Biot [20] which focused on poroelasticity for geomechanics. Others following the work of Truesdell [21], Bowen [22] and Shi et al. [23] are based on the theory of mixtures. Recent models using these approaches have found success in modeling the behavior of swollen elastomers [24,25]. Lastly, Bouklas and Huang [26] have demonstrated that a linear poroelasticity theory is consistent with the Flory–Rehner theory under the condition of small perturbations from a freely swollen state. However, in what follows we take the approach of extending the Flory–Rehner theory to account for limiting chain extensibility. It is worthwhile to elucidate the interaction between limiting chain extensibility and swelling in swollen elastomers undergoing finite deformations because a more comprehensive analysis may provide a deeper interpretation to the mechanical and swelling behavior of gels, such as pH sensitive hydrogels with very large swelling ratios.

In this study, ultimate swelling characterized by limiting chain extensibility of swollen elastomers is examined. Section 2 presents the fundamental relations derived from the Flory–Rehner theory. Limiting chain extensibility is introduced via the AB and G models. The difference between these models is unified by defining a single scalar function. Section 3 shows that an inequality is derived from the limit included in this scalar function, which is used for ultimate analysis in Sections 4 and 5. The ultimate

analysis is performed under free swelling and uniaxial loading, respectively, which yields an ultimate value of the volume swelling ratio. This ultimate value is not exceeded at equilibrium swelling regardless of the set of material constants. Under uniaxial loading at equilibrium swelling, deswelling can occur even in tension. Further, in Section 6, the very large swelling behavior of pH sensitive hydrogels is found to result from the resistance generated by approaching the ultimate value of swelling. Finally, conclusions are presented in Section 7.

2. Fundamental relations

Flory and Rehner [5] assumed that to describe the mechanical and swelling behavior of elastomers, the free energy function is expressed as the sum of two terms associated with polymer stretching and the mixing of polymer and solvent molecules:

$$W = W_{\mathrm{e}}(\lambda_i) + W_{\mathrm{m}}(C)\,, \tag{1}$$

where W_{e} is the elastic strain energy and W_{m} is the mixing energy. The use of the Gaussian network theory and the Flory–Huggins solution theory gives:

$$W_{\mathrm{e}} = \frac{E_0}{6}(I_1 - 3 - a\log J)\,, \quad \text{Neo–Hookean (NH) model,} \tag{2}$$

$$W_{\mathrm{m}} = -\frac{kT}{\upsilon}\left\{\upsilon C\log\left(1+\frac{1}{\upsilon C}\right)+\frac{\chi}{1+\upsilon C}\right\}, \tag{3}$$

where λ_i (i = 1, 2, 3) are the principal stretches so that the invariants are expressed as $I_1 = \lambda_1^2 + \lambda_2^2 + \lambda_3^2$, $I_2 = \lambda_1^2\lambda_2^2 + \lambda_2^2\lambda_3^2 + \lambda_3^2\lambda_1^2$ and $J = \lambda_1\lambda_2\lambda_3$, and C is the nominal concentration of solvent molecules.

In Eq. (2), E_0 is the reference Young's modulus. For the NH model, E_0 is defined as the Young's modulus of the undeformed, unswollen state (i.e., $\lambda_i = 1$). The logarithmic term $-a \log J$ originates from the entropy of deformation [1]. The value of a depends on the theory and can be taken as a = 0, 1 and 2 [1,2,7,27]. It is also possible to take a

negative value to describe phenomenologically the experimental data [28]. This logarithmic term will be introduced into the AB and G models in the same manner. However, for simplicity, $a = 0$ is used as the representative value (see Appendix A). In Eq. (3), kT is the absolute temperature expressed as a thermal energy, υ is the volume per solvent molecule, and χ is the Flory–Huggins interaction parameter that characterizes the enthalpy of mixing.

When the NH model is replaced by the AB or G models including the non-Gaussian chain effect, W_e for the AB model [11] is expressed as:

$$W_e = \frac{E_0}{6}\left\{2\sqrt{n}\beta\Lambda + 2n\log\left(\frac{\beta}{\sinh\beta}\right) - a\log J\right\}, \quad \text{Arruda–Boyce (AB) model,} \tag{4}$$

where n is the number of rigid links in the single chain related to limited extensibility, and

$$\Lambda = \sqrt{(\lambda_1^2 + \lambda_2^2 + \lambda_3^2)/3} = \sqrt{I_1/3}, \tag{5}$$

$$\beta = L^{-1}(\Lambda/\sqrt{n}). \tag{6}$$

Here, $L^{-1}(x)$ is the inverse Langevin function defined as $x = \coth\beta - 1/\beta = L(\beta)$. In contrast, W_e for the G model [12] is expressed as:

$$W_e = \frac{E_0}{6}\left\{-J_m\log\left(1 - \frac{I_1 - 3}{J_m}\right) - a\log J\right\}, \quad \text{Gent (G) model,} \tag{7}$$

where J_m is a material constant to describe the limiting chain extensibility. When Eqs. (4) and (7) take the limit as $n \to \infty$ and $J_m \to \infty$, respectively, the AB and G models reduce to the NH model [14].

In the AB model, the effect of limiting chain extensibility is described as a process where $L^{-1}(x)$ takes the limit as $x \to 1$, i.e., $\beta \to \infty$. Note that $L^{-1}(x)$ cannot be written in a closed form and this feature prevents further analytical analysis [29]. To avoid this problem simply, the Padé approximant can be used to approximate the inverse Langevin

function [30], that is,

$$\beta = L^{-1}(x) \approx 3x\frac{35-12x^2}{35-33x^2}, \quad \text{Padé (P) approx.} \tag{8}$$

Eq. (8) is a simple form and is able to take the limit as $x \to (35/33)^{1/2} \approx 1.03$, leading to $\beta \to \infty$ (cf. a truncation of the Taylor series of $L^{-1}(x)$). Thus, the employment of Eq. (8) makes analytical manipulation easy using the AB model. In addition, the G model takes the limit as $I_1 \to 3 + J_m$ (see Eq. (7)). Although there are different approximations originating from the Padé approximant [14,29,30], the present study simply focuses on Eq. (8) as a standard case.

Assuming that the network of polymer and liquid solvent is incompressible, the volume of swollen elastomers is the sum of the volume of the dry network and that of the swelling solvent [2,6]. The volume swelling ratio of swollen elastomers is equal to J and is expressed as

$$J = 1 + \upsilon C. \tag{9}$$

When a Lagrange multiplier is used in Eq. (1) to impose the constraint of Eq. (9),

$$W = W_e(\lambda_i) + W_m(C) + \Pi(1 + \upsilon C - J), \tag{10}$$

where Π is the Lagrange multiplier, and is referred to as the osmotic pressure due to mixing in the present study [7,31,32].

Eq. (10) gives the nominal stress in each direction of the principal stretches (i = 1, 2, 3),

$$s_i = \frac{\partial W}{\partial \lambda_i} = \frac{E_0}{3}\left(\Omega\lambda_i - \frac{a}{2\lambda_i}\right) - \Pi\frac{J}{\lambda_i}, \tag{11}$$

where Ω is the scalar function that depends on the models (Eqs. (2), (4) and (7)), that is,

$$\Omega(I_1)=\begin{cases} 1 & \text{, NH model} \\ \dfrac{\sqrt{n}\beta}{3\Lambda} & \text{, AB model} \\ \dfrac{35n-4I_1}{35n-11I_1} & \text{, AB model+P approx.} \\ \dfrac{J_{\mathrm{m}}}{J_{\mathrm{m}}-I_1+3} & \text{, G model} \end{cases}. \tag{12}$$

The nominal stress of Eq. (11) is transformed into the true stress,

$$\sigma_i=\frac{s_i\lambda_i}{J}=\frac{E_0}{3J}\left(\Omega\lambda_i^{\,2}-\frac{a}{2}\right)-\Pi\,, \quad \text{no sum on } i. \tag{13}$$

Eqs. (11) and (13) imply that the difference between the models is unified via the single scalar function Ω. Next, when μ presents the chemical potential of the external solvent, Eqs. (3), (9) and (10) lead to

$$\mu=\frac{\partial W}{\partial C}=kT\left\{\log\left(\frac{J-1}{J}\right)+\frac{1}{J}+\frac{\chi}{J^2}\right\}+\Pi\upsilon=0. \tag{14}$$

Eq. (14) indicates that μ is balanced with the chemical potential in swollen elastomers, and the elastic contribution is introduced via the Lagrange multiplier Π (i.e., the osmotic pressure). At equilibrium swelling ($\mu = 0$), the elastic contribution (i.e., Π) is balanced with the mixing contribution in swollen elastomers.

In Eq. (14), $\mu = 0$ expresses the state in which the network of polymers is in contact with the liquid solvent [6,7,9,33,34]. When p and p_0 are the pressure of the external solvent and the vapor pressure of the solvent, respectively, $\mu = (p - p_0)\upsilon$ under $p \geq p_0$ and $\mu = kT \log (p / p_0)$ under $p < p_0$. In a vacuum ($p = 0$), $\mu = -\infty$ is consistent with $J = 1$ in Eq. (14) and $C = 0$ from Eq. (9), i.e., the network of polymers is in the dry state. Further, since the contribution of the differential pressure between the vapor pressure and the atmospheric pressure is relatively small [9,35], $\mu = 0$ can be regarded as the equilibrium swelling state in practice [6,7,9,33,34]. As the value of μ increases from $-\infty$ to 0, the value of J increases from 1 to a value that obeys Eq. (14). Here, Π depends on

the type of external forces, i.e., Eq. (13).

3. Ultimate condition

Ultimate analysis is performed by considering the limit included in the scalar function Ω for the AB, AB+P and G models; i.e., Eq. (12) yields an inequality as follows

$$0 < \begin{cases} 3n - I_1 & \text{, AB model} \\ 35n - 11I_1 & \text{, AB model+P approx.,} \\ J_m - I_1 + 3 & \text{, G model} \end{cases} \tag{15}$$

which is not novel for providing the limiting stretches of elastomers that depend on the type of external forces, such as uniaxial and biaxial extensions. However, *in the present study, Eq. (15) is analyzed to describe the ultimate swelling of swollen elastomers undergoing finite deformations.* As expected, the first invariant, $I_1 = \lambda_1^2 + \lambda_2^2 + \lambda_3^2$, must obey this inequality. The ultimate value of I_1, which is also related to the ultimate value of J because $J = \lambda_1 \lambda_2 \lambda_3$, is found to be restricted only to the material constant that describes limited extensibility, that is, n and J_m for the AB and G models, respectively. Since a change of J is caused by swelling (Eq. (9)), Eq. (15) is expected to impose a considerable restriction on the swelling behavior of elastomers.

Eqs. (12) and (15) show that $\Omega \to \infty$ when $I_1 \to 3n$ for the AB model, $I_1 \to (35/11)n$ for the AB+P model and $I_1 \to J_m + 3$ for the Gent model. Thus, when the limits of Ω (i.e., $\Omega \to \infty$) for the individual models occur at the same value of I_1, the AB, AB+P and G models have an equivalent expression between n and J_m [14]:

$$J_m = \begin{cases} 3n - 3 & \text{, AB model,} \\ \frac{35}{11}n - 3 & \text{, AB model+P approx.} \end{cases} \tag{16}$$

Fig. 1 shows that if Eq. (16) is applied, the limit of I_1 predicted by the G model is equal to that predicted by the AB and AB+P models, respectively. A slight difference in the

overall profiles remains between the AB and G models even when the Padé approximant is used [13,14]. The G model has a tendency to predict a slightly larger value compared to the AB model for the scalar function Ω at intermediate values of I_1. If a different approximation originating from the Padé approximant are used [14,29,30], this tendency can change depending on the approximation. However, the ultimate analysis in Sections 4 and 5 is based on Eq. (15) and is not affected by this slight difference. Thus, as will be shown in Section 4, if Eq. (16) is used, the AB and G models provide identical predictions for ultimate analysis (Fig. 3).

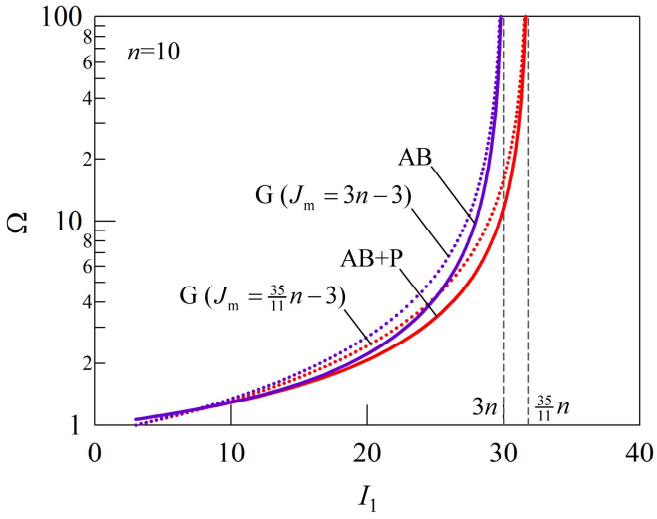

Fig. 1. Overall profile of the scalar function Ω as a function of the invariant I_1 for n = 10 and the limit value of I_1. The G model can be adjusted to take the same limit value as the AB and AB+P models by using Eq. (16).

The present study focuses on two typical states, free swelling (Section 4) and uniaxial tension and compression (Section 5), to perform ultimate analysis using Eq. (15). Eq. (15) shows that the ultimate value of I_1 depends only on n or J_m. The type of external forces needed to determine the set of principal stretches results in the characterization of the ultimate value of J. Thus, the ultimate values of J under free swelling and uniaxial loading are independent of the combination of other material constants, such as E_0, a, χ, υ and kT. In contrast, when equilibrium swelling is analyzed using Eq. (14), the value of J is dependent on all material constants and the type of external forces. *Thus, the volume swelling ratio at equilibrium swelling is expected not*

to exceed the ultimate value obtained by ultimate analysis using Eq. (15). In Sections 4 and 5, the responses at ultimate swelling are compared with those at equilibrium swelling. Fig. 2 shows schematic illustrations of the states of equilibrium free swelling (Fig. 2b) and uniaxial extension at equilibrium swelling (Fig. 2c). In these states, the relations of stresses and stretches are also written in Fig. 2.

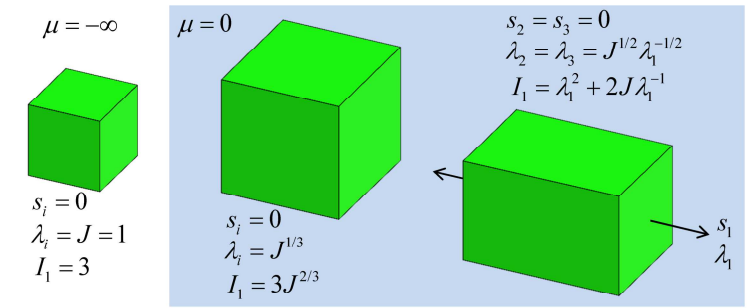

(a) Initial state (b) Free swelling (c) Uniaxial loading

Fig. 2. Schematic illustrations of (a) the initial, undeformed dry state, (b) equilibrium free swelling and (c) uniaxial extension at equilibrium swelling. At equilibrium swelling ($\mu = 0$), Eq. (14) determines J and is dependent on all material constants and the type of external forces via Π.

4. Analysis under free swelling

Regardless of attaining equilibrium swelling ($\mu = 0$), the free swelling state is characterized by isotropic stretches and the absence of stresses (Fig. 2b), that is,

$$\begin{cases} s_1 = s_2 = s_3 = 0 \\ \lambda_1 = \lambda_2 = \lambda_3 = J^{1/3} \end{cases}, \text{ under free swelling.} \tag{17}$$

Since this state takes $I_1 = 3J^{2/3}$, the inequality of Eq. (15) reduces to

$$J < J_{\text{ult}} = \begin{cases} n^{3/2} & , \text{AB model} \\ \left(\frac{35}{33}n\right)^{3/2} & , \text{AB model+P approx.}, \\ \left(\frac{1}{3}J_{\text{m}} + 1\right)^{3/2} & , \text{G model} \end{cases} \tag{18}$$

where J_{ult} is the ultimate value of the volume swelling ratio under free swelling, which has a very simple form depending on n or J_m. Eq. (18) results from the limit due to limiting chain extensibility. The volume swelling ratio at equilibrium free swelling cannot exceeds this ultimate value that is independent of the set of material constants except for n or J_m.

Fig. 3 shows the comparison of the different models according to Eq. (18). The G model gives the same value with the AB and AB+P models using the equivalent relation of Eq. (16). The difference between the AB and AB+P models is also found to be very small (Figs. 1 and 3). The AB+P model overestimates J_{ult} predicted by the AB model by ~9%. The factor generating this deviation is clear (i.e., $1 \approx 35/33$ in Eq. (18)). Thus, in the following sections, we mainly analyze the AB+P model to investigate the effects of limiting chain extensibility because this model is written in the closed form with the Padé approximant (see Eq. (12) for the AB model), and the physical meaning of n is clear.

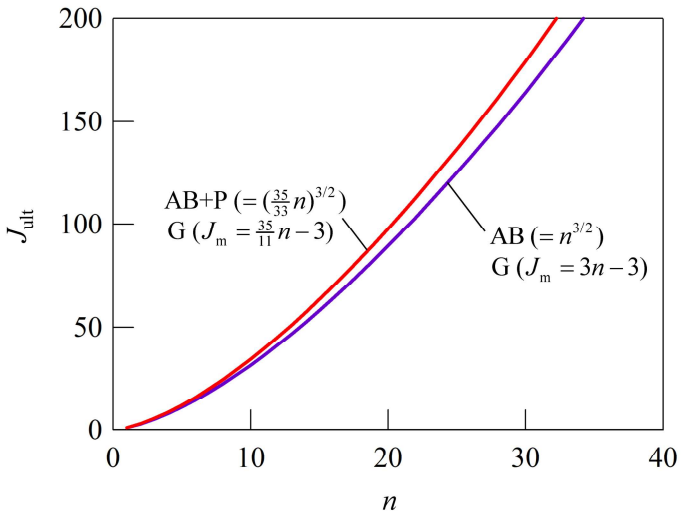

Fig. 3. Ultimate value, J_{ult}, of the volume swelling ratio under free swelling. The value only depends on n or J_m with the very simple form. The volume swelling ratio at equilibrium free swelling cannot exceed this ultimate value that is independent of a set of material constants, except for n or J_m.

When equilibrium swelling is considered under free swelling (Fig. 2b), Eq. (17) is

first used to obtain the osmotic pressure Π from Eq. (13):

$$\Pi = \frac{E_0}{3}\left(\Omega J^{-1/3} - \frac{a}{2J} \right), \tag{19}$$

which is the elastic contribution in Eq. (14). Substituting this expression into Eq. (14) yields

$$\left\{ \log\left(\frac{J-1}{J} \right) + \frac{1}{J} + \frac{\chi}{J^2} \right\} + \frac{E_0 \upsilon}{3kT}\left(\Omega J^{-1/3} - \frac{a}{2J} \right) = 0 . \tag{20}$$

By solving this equation, the volume swelling ratio J at equilibrium swelling is obtained, which is a function of the material constants, χ, $E_0\upsilon/(3kT)$, a and Ω, including n or J_m. Here, $E_0\upsilon/(3kT)$ is regarded as the non-dimensional material constant related to the Young's modulus. According to Eq. (18), J cannot exceed the ultimate value J_{ult}.

When a parameter of $\phi < 1$ is introduced to define the ratio of J to J_{ult}, i.e., $\phi = J/J_{ult}$, the volume swelling ratio at equilibrium swelling for the AB+P model is expressed as

$$J_\phi = \phi\left(\frac{35n}{33} \right)^{3/2} . \tag{21}$$

Using Eq. (21), the scalar function Ω (Eq. (12)) is reduced to

$$\Omega_\phi = \frac{1 - \frac{4}{11}\phi^{2/3}}{1 - \phi^{2/3}}, \tag{22}$$

and Eqs. (21) and (22) give a transformed expression of Eq. (20):

$$\left\{ \log\left(\frac{J_\phi - 1}{J_\phi} \right) + \frac{1}{J_\phi} + \frac{\chi}{J_\phi^2} \right\} + \frac{E_0 \upsilon}{3kT}\left(\frac{1 - \frac{4}{11}\phi^{2/3}}{1 - \phi^{2/3}} J_\phi^{-1/3} - \frac{a}{2J_\phi} \right) = 0 . \tag{23}$$

Fig. 4 is obtained by plotting Eq. (23), which shows the combination of $E_0\upsilon/(3kT)$ and n that is required to increasing ϕ to 1, i.e., increasing J to J_{ult}, at equilibrium free

swelling. Fig. 5, which is obtained by solving Eq. (20), shows the dependence on the interaction parameter χ. It is clearly demonstrated that in a good solvent ($\chi < 0.5$), as $E_0\upsilon/(3kT)$ decreases, the volume swelling ratio at equilibrium free swelling approaches the ultimate value J_{ult}. Although for the NH model, J increases monotonically as χ decreases, the approach to J_{ult} prevents a further increase of J for a smaller value of $E_0\upsilon/(3kT) = 10^{-5}$ (Fig. 5).

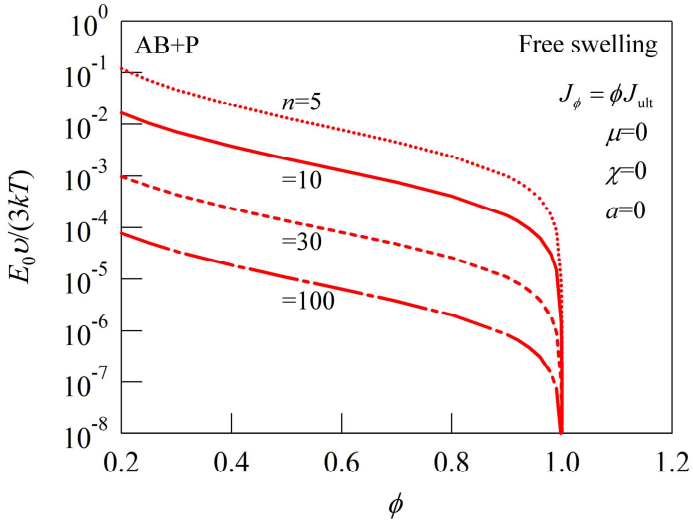

Fig. 4. Combination of $E_0\upsilon/(3kT)$ and n needed to attain J_ϕ at equilibrium free swelling for $\chi = 0$ and $a = 0$. To approach the ultimate value as $\phi = 1$, $E_0\upsilon/(3kT)$ is required to be smaller as n increases.

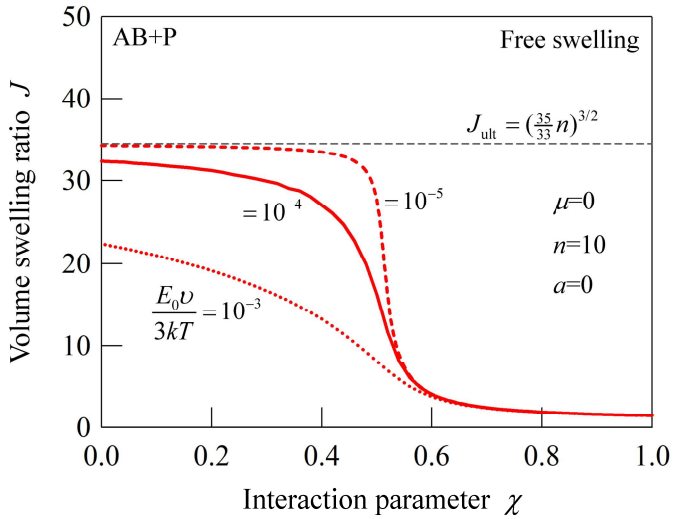

Fig. 5. Volume swelling ratio J at equilibrium free swelling as a function of the interaction parameter χ for $n = 10$ and $a = 0$. As $E_0\upsilon/(3kT)$ decreases, J approaches the ultimate value of J_{ult} in a good solvent ($\chi < 0.5$).

Moreover, for example, to attain $\phi = 0.9$ in Fig. 4, $E_0\upsilon/(3kT) = 10^{-3}$ is roughly needed for $n = 5$, $E_0\upsilon/(3kT) = 10^{-5}$ for $n = 30$ and $E_0\upsilon/(3kT) = 10^{-6}$ for $n = 100$. Since hydrogels are at room temperature, the solvent is just water, i.e., $\upsilon \approx 3\times10^{-29}(\mathrm{m}^3)$ and $kT \approx 4\times10^{-21}(\mathrm{J})$, the reference Young's modulus needed is $E_0 = 400$–0.4 (kPa) for $n = 5$–100. These values are normal for realistic hydrogels [15,17,36,37]. This fact indicates the necessity to introduce the effect of limiting chain extensibility in the Flory–Rehner theory to describe the mechanical and swelling behavior of hydrogels. Further discussion will be given in Section 6 using experimental data of pH sensitive hydrogels, whereas in Section 5 responses under uniaxial loading are investigated.

5. Analysis under uniaxial loading

Despite attaining equilibrium swelling ($\mu = 0$), the uniaxial loading state in the x_1 direction is characterized by

$$\begin{cases} s_2 = s_3 = 0 \\ \lambda_2 = \lambda_3 = J^{1/2}\lambda_1^{-1/2} \end{cases}, \text{ under uniaxial loading in } x_1 \text{ direction,} \tag{24}$$

which leads to $I_1 = \lambda_1^2 + 2J\lambda_1^{-1}$, and thus the inequality of Eq. (15) is rewritten as

$$J < \begin{cases} \frac{1}{2}\lambda_1(3n - \lambda_1^2) & \text{, AB model} \\ \frac{1}{2}\lambda_1(\frac{35}{11}n - \lambda_1^2) & \text{, AB model+P approx.} \\ \frac{1}{2}\lambda_1(J_\mathrm{m} + 3 - \lambda_1^2) & \text{, G model} \end{cases}. \tag{25}$$

The ultimate value of the volume swelling ratio under uniaxial loading is a function of not only n or J_m, but also λ_1. It is trivial that if $\lambda_1 = J^{1/3}$, Eq. (25) is reduced to Eq. (18) under free swelling (i.e., Eq. (25) includes Eq. (18)). In addition, $J \geq 1$ is needed because $J = 1$ expresses the dry state in the absence of solvent molecules. Thus, the combination of J and λ_1 exists only in the domain surrounded by Eq. (25) and $J \geq 1$ (Fig. 6).

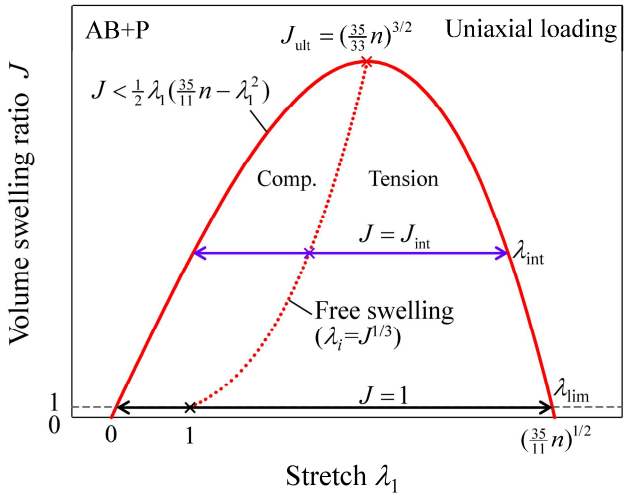

Fig. 6. Interaction between the two different limit values of J and λ_1 under uniaxial loading. The combination of J and λ_1 exists only in the domain surrounded by Eq. (25) and J = 1. The maximum value of J is equal to J_{ult} under free swelling. If n is sufficiently large, $\lambda_{lim} \approx (35n/11)^{1/2}$ and λ_{int} exists over the range of $(35n/33)^{1/2} < \lambda_{int} < \sqrt{3}(35n/33)^{1/2}$ for the AB+P model.

Fig. 6 illustrates that Eq. (25) gives a very distinct interpretation to the effect of limiting chain extensibility on the interaction between the two different limits of J and λ_1 of swollen elastomers. The surrounded domain is divided into tensile and compressive domains, of which the boundary expresses the free swelling state ($\lambda_1 = J^{1/3}$). Thus, the maximum value of J is found to be the ultimate value of J_{ult} under free swelling (Eq. (18)). When J = 1 is fixed during uniaxial loading, the limits of λ_1 in the tensile and compressive directions are expressed as the two points at which Eq. (25) and J = 1 intersect. Next, when an intermediate volume swelling ratio J_{int} between $1 < J_{int} < J_{ult}$ is selected, the two limit points in the two directions are also obtained using Eq. (25). Here, the limit points of λ_1 in the tensile direction are referred to as λ_{lim} and λ_{int} for J = 1 and J_{int}, respectively (Fig. 6). It is clear that the limit point of λ_{int} is in the range between $J_{ult}^{1/3} \le \lambda_{int} \le \lambda_{lim}$. As J_{int} increases from 1 to J_{ult}, λ_{int} decreases from λ_{lim} to $J_{ult}^{1/3}$. The point of $J_{int} = J_{ult}$ is singular because $\lambda_{int} = J_{ult}^{1/3}$ means that when $J_{int} = J_{ult}$ is fixed, there cannot be any stretch except $\lambda_1 = J_{ult}^{1/3}$.

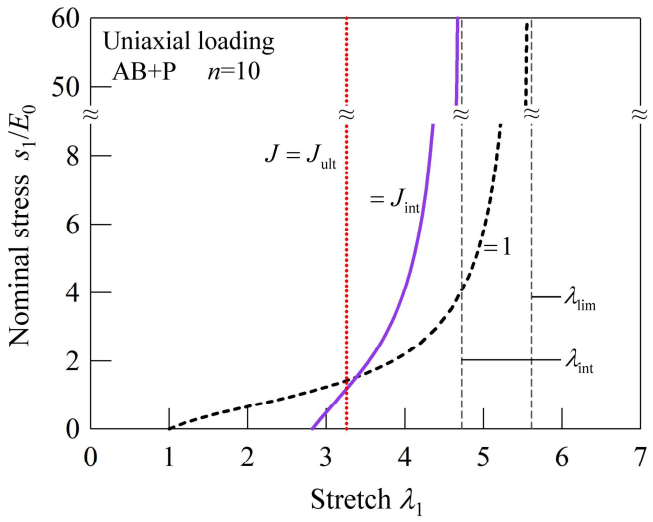

Fig. 7. Stress–stretch response under uniaxial tension for n = 10 when the volume swelling ratio is fixed as J = 1, J_{int} = 22.4, and $J_{ult} = (35n/33)^{3/2}$ = 34.54. The effect of limiting chain extensibility on swollen elastomers appears as a process where J approaches J_{ult}.

To understand the above-mentioned singular point, the stress–stretch responses under uniaxial tension with a constant value of J = 1, J_{int} and J_{ult} are plotted using the following relation

$$s_1 = \frac{E_0}{3}\Omega(\lambda_1 - \lambda_1^{-1}\lambda_3^2) = \frac{E_0}{3}\Omega(\lambda_1 - J\lambda_1^{-2}), \tag{26}$$

which is derived from Eqs. (11), (13) and (24). Fig. 7 shows that at J=J_{ult}, I_1 and J have no combination except for that of J=J_{ult} and $\lambda_1 = \lambda_2 = \lambda_3 = J_{ult}^{1/3}$, resulting in a steep increase in the stress with an infinitely large gradient. As J decreases from J_{ult} to 1, the limit value of the stretch can be taken as a value larger than $\lambda_1 = J_{ult}^{1/3}$, whereas the stretch at $s_1 = 0$ can be taken as a value smaller than $\lambda_1 = J_{ult}^{1/3}$. As a result, a familiar profile of elastomers appears in the response. In particular, the profile of J = 1 shows the response of the elastomer in the absence of solvent molecules [2,11]. In conclusion, swelling (i.e., increasing J from 1) increases the apparent stiffness and decreases the apparent limit stretch as the effect of limiting chain extensibility. This mechanism appears as a process where J approaches J_{ult}.

Although Figs. 6 and 7 clearly show the interaction between swelling and stretches

that occurs under uniaxial loading, the volume swelling ratio J can change to maintain equilibrium swelling ($\mu = 0$). Thus, the interaction at equilibrium swelling under uniaxial loading is analyzed here. To consider equilibrium swelling, Eq. (26) must be solved with Eq. (14). Under uniaxial loading, Eqs. (13) and (24) give the osmotic pressure Π, which is substituted into Eq. (14):

$$\left\{\log\left(\frac{J-1}{J}\right)+\frac{1}{J}+\frac{\chi}{J^2}\right\}+\frac{E_0\upsilon}{3kT}\left(\Omega\lambda_1^{-1}-\frac{a}{2J}\right)=0. \tag{27}$$

Eq. (27) is solved to obtain J when λ_1 is given. The stress–stretch response at equilibrium swelling is estimated via Eq. (26). In Eq. (27), if $\Omega = 1$ (i.e., the NH model), an increase of λ_1 causes a decrease of the elastic contribution, which causes an additional amount of swelling. As stated in Treloar [2], J increases under uniaxial tension. However, when Ω takes the limit, i.e., $\Omega \to \infty$, for the AB, AB+P and G models, this change can cause an opposite reaction to the increase of λ_1. In other words, the elastic contribution of the second term in Eq. (27) is expected to increase dramatically as $\Omega \to \infty$.

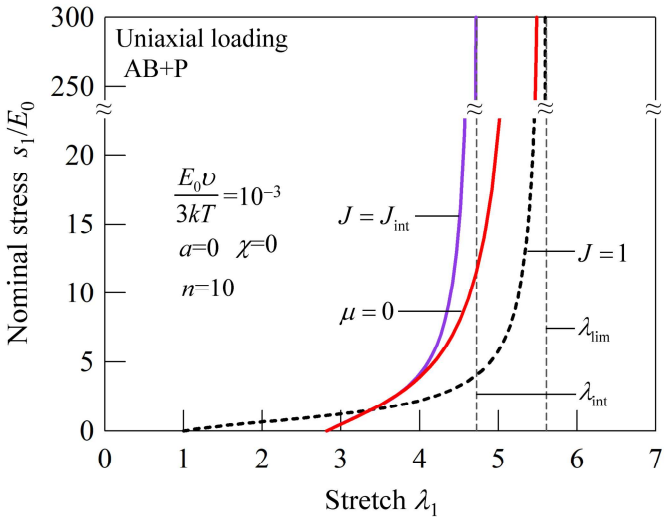

Fig. 8. Effect of equilibrium swelling ($\mu = 0$) on the stress–stretch response under uniaxial tension for $E_0\upsilon/(3kT) = 10^{-3}$, $n = 10$, $\chi = 0$ and $a = 0$. To compare the responses of $J = J_{int}$ and $\mu = 0$, $J_{int} = 22.4$ was selected to take the same value of λ_1 at $s_1 = 0$. At equilibrium swelling, limiting chain extensibility causes deswelling even under tension. The response of $\mu = 0$ exceeds the limit line of λ_{int} and approaches the limit line of λ_{lim}.

To investigate this limiting chain effect, Fig. 8 shows the comparison of the responses for $J = J_{\text{int}}$ and $\mu = 0$, where $J_{\text{int}} = 22.4$ was selected to take the same value of λ_1 at $s_1 = 0$. The response of $\mu = 0$ starts to deviate from that of $J = J_{\text{int}}$ around $\lambda_1 = 4$. This deviation originates from the change of J. If an additional amount of swelling occurs, the response of $\mu = 0$ cannot exceed the limit line of λ_{int} because the increase of J decreases the value of λ_{int} (Fig. 6). However, interestingly, the response not only exceeds the limit of λ_{int} but also approaches the limit of λ_{lim}. This is only interpreted by the occurrence of deswelling to $J = 1$. Uniaxial tension is generally expected to increase J at equilibrium swelling [2]. In fact, the effect of limiting chain extensibility induces deswelling when approaching the limit of λ_{lim}.

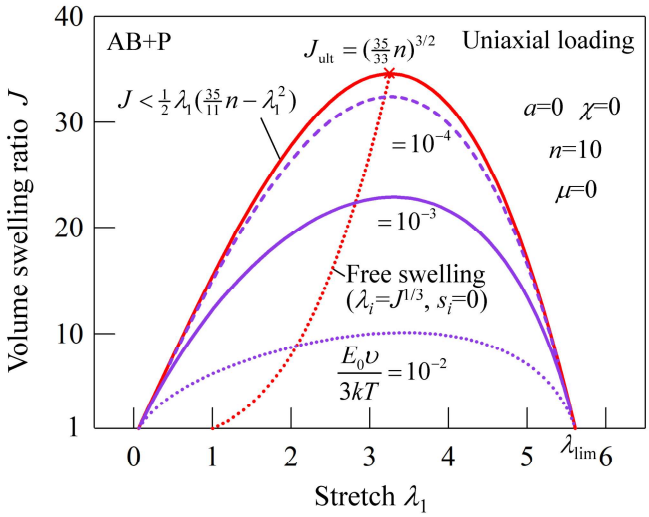

Fig. 9. Effect of equilibrium swelling ($\mu = 0$) on the change of J under uniaxial tension and compression for $E_0\upsilon/(3kT) = 10^{-2}$, 10^{-3} and 10^{-4}, $n = 10$, $\chi = 0$ and $a = 0$. The profiles are in the domain surrounded by Eq. (25) and $J = 1$. Under tension, although J first increases slightly, after that, J decreases to 1 because of the effect of limiting chain extensibility (i.e., deswelling occurs).

Fig. 9 shows the change of J under uniaxial loading at equilibrium swelling for different values of $E_0\upsilon/(3kT)$, which is plotted in Fig. 6. The change of J at equilibrium free swelling corresponds with that described in Fig. 5; i.e., a smaller value of the Young's modulus increases J at equilibrium free swelling. The response approaches the

point of J_{ult}. Fig. 9 also shows that the profiles are in the domain surrounded by the two limits described by Eq. (25) and $J = 1$ and the deswelling to $J = 1$ on both sides of tension and compression. As $E_0\upsilon/(3kT)$ increases, J at equilibrium swelling first increases slightly under tension. This is a well-known effect stated in Treloar [2]. However, subsequently, J starts to decrease to 1 when approaching $\lambda_l \rightarrow \lambda_{lim}$. This deswelling behavior is found to occur as an effect of limiting chain extensibility at equilibrium swelling, regardless of the value of $E_0\upsilon/(3kT)$.

6. Interpretation of the response of pH sensitive hydrogels

Here, the mechanism originating from ultimate swelling is demonstrated to play an essential role in causing the very large swelling behavior of pH sensitive hydrogels. To this end, the experiments performed by Li et al. [17] and Ricka and Tanaka [38] are focused on. In their experiments, a polyacrylamide-co-acrylic acid hydrogel was used as a polyelectrolyte gel, which has the ability to attain very large swelling ratios depending on changes in pH and salinity of the external solvent; i.e., J can exceed 1000. Their two different pH sensitive hydrogels are simply distinguished as Li's and Tanaka's gels, respectively.

Li et al. [17] reported that at very large swelling ratios, the osmotic pressure due to mobile ions, Π_{ion}, is dominant when compared with that due to mixing, Π_{mix}, and the introduction of the non-Gaussian chain effect becomes important to estimate a unified master curve of Π_{mix} instead of using the Flory–Huggins solution theory. The discrepancy generated by the Gaussian network theory (i.e., the NH model) at very large swelling ratios can be removed using the Gent model with an appropriate value of J_m. In this section, a more comprehensive interpretation is provided by paying attention to the mechanism of ultimate swelling (Section 4) and the interaction of Π_{ion} with limiting chain extensibility.

According to Marcombe et al. [39] and Li et al. [17], the contribution of Π_{ion} can be added in the true stress expression (Eq. (13)),

$$\sigma_i = \frac{E_0}{3J}\left(\Omega\lambda_i^2 - \frac{a}{2}\right) - \Pi_{\mathrm{mix}} - \Pi_{\mathrm{ion}}, \tag{28}$$

where Π_{mix} is equal to Π in Eq. (13), which is derived from Eq. (14). Under equilibrium free swelling $\sigma_i = 0$ and $\lambda_i = J^{1/3}$ in Eq. (28). Thus,

$$\Pi_{\mathrm{mix}} = \frac{E_0}{3}\left(\Omega J^{-1/3} - \frac{a}{2J}\right) - \Pi_{\mathrm{ion}}. \tag{29}$$

Here, Π_{mix} decreases monotonically from ∞ to 0 as J increases from 1 (Eq. (14)). Li et al. (2014) also confirmed in their experimental approach that Π_{mix} shows a monotonic decrease with increasing J. When Π_{mix} is balanced with two terms owing the elastic and ionic contributions (Eq. (29)), J is estimated as a value at equilibrium swelling. The elastic term in Eq. (29) consists of Ω including the effect of limiting chain extensibility (Eq. (12)), while Π_{ion} is a positive value calculated from the individual concentrations of mobile ions in the external solvent [17,39]. The increase in Π_{ion} increases J of pH sensitive hydrogels. In the present study, instead of calculating the value of Π_{ion} from each concentration, the value of Π_{ion} is changed directly as a parameter; i.e., Π_{ion} is increased from 0. This simple approach allows us to investigate the transient response that approaches to the ultimate value of swelling, J_{ult}, under free swelling (see Section 4).

First of all, $\Pi_{ion} = 0$ is considered to show the elastic contribution in Eq. (29), which includes the effect of limiting chain extensibility on Π_{mix}. Fig. 10 shows the comparison of the NH and G models. The value of $J_m = 260$ for the G model was estimated as the value fitted by experiments of the gel tagged with AA04-433 [17]. The introduction of limiting chain extensibility gives the ultimate value of swelling, $J_{ult} = 820$ (Eq. (18)). As J increases to J_{ult}, a larger value of Π_{mix} is needed to attain equilibrium swelling. Consequently, Li's gel had a volume swelling ratio between $30 < J < 350$. The effect of limited extensibility is quantified as the additional increase of Π_{mix} between the NH and G models. If this additional increase of Π_{mix} is absent (i.e., if the NH model is used), the experimentally measured osmotic pressure of Π_{mix} becomes negative at J = 200–350 so that Li et al. [17] concluded that the additional increase of Π_{mix} because of the non-Gaussian chain effect is important to obtain a unified master curve of Π_{mix} applied for a series of the gels having different values of the Young's modulus. Incidentally, a =

0 is simply selected in the present study to discuss the effect of $J_m = 260$, whereas Li et al. (2014) used $a = 2$, but the influence is negligible at $J > 20$ (see Appendix A).

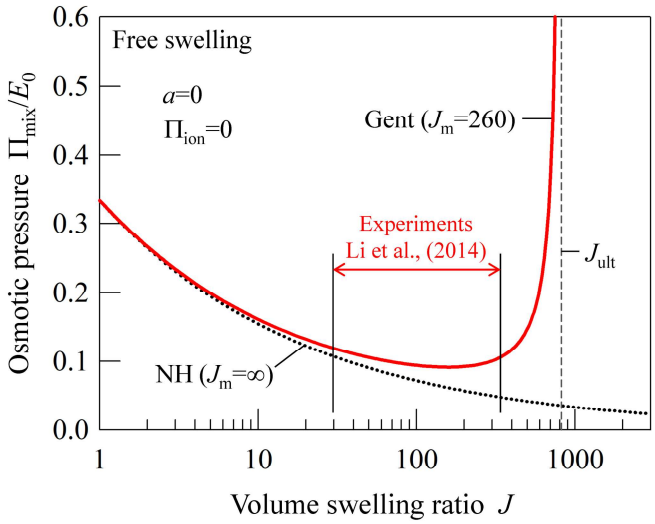

Fig. 10. Elastic contribution to the osmotic pressure due to mixing predicted by the NH and G models with $\Pi_{ion} = 0$ and $a = 0$. Li et al. [17] determined $J_m = 260$ to obtain a unified master curve of Π_{mix}. The value of Π_{mix} increases steeply as J approaches the ultimate value of $J_{ult} = 820$, whereas the NH model predicts a monotonic decrease in Π_{mix}.

Although Li's gel needed the Gent model to obtain the experimentally measured master curve of Π_{mix}, the present study uses Π_{mix} derived from the Flory–Huggins solution theory (i.e., Eqs. (3) and (14)) to elucidate the effect of limiting chain extensibility on pH sensitive hydrogels with very large swelling ratios. Thus, when Π in Eq. (14) is substituted into Π_{mix} in Eq. (29),

$$\left\{\log\left(\frac{J-1}{J}\right)+\frac{1}{J}+\frac{\chi}{J^2}\right\}+\frac{E_0\upsilon}{3kT}\left(\Omega J^{-1/3}-\frac{a}{2J}-\frac{3\Pi_{ion}}{E_0}\right)=0\,, \tag{30}$$

which is the balance equation extended by Π_{ion} (cf. Eq. (20)) and is solved to estimate J under equilibrium free swelling as a function of Π_{ion}. For Li's gel (AA04-433), the material constants were measured as $E_0 = 52.17$ (kPa) and $J_m = 260$ as well as $J = 61$ at $\Pi_{ion} = 1550$ (Pa) in distilled water at pH = 6.5. The use of $kT = 4\times10^{-21}$ (J) and $\upsilon = 3\times10^{-29}$ (m^3) gives $E_0\upsilon/(3kT) = 1.30\times10^{-4}$. Thus, when $a = 0$ (see Appendix A), χ is determined to fit Eq. (30) to the condition of $J = 61$ at $\Pi_{ion} = 1550$ (Pa). Consequently,

the G model with $J_m = 260$ needs $\chi = 0.40$, whereas if the NH model is assumed, $\chi = 0.426$. Here, χ was only used as a fitted parameter [2,32].

Fig. 11 shows the changes of J and Π_{ion} predicted from Eq. (30). If the Gent model is used, the increase of Π_{ion} causes the monotonic increase of J and finally approaches J_{ult}. An inverted S shape appears in the profile of Fig. 11. In their experiments, when the gel was immersed in alkaline solutions (pH > 7), J increased up to approximately 350, whereas under acidic conditions (pH < 7), J decreased down to approximately 30. The predicted response between J and Π_{ion} in this range shows a similar tendency to that observed in experiments [17]. It is very important to note that the NH model predicts the gel to be dissolved when Π_{ion}/E_0 is larger than approximately 0.05. This means that the NH model cannot explain even the qualitative response of pH sensitive hydrogels. Thus, the effect of limiting chain extensibility plays an essential role in causing the very large increase of J as Π_{ion} increases for pH sensitive hydrogels. *The very large swelling behavior of pH sensitive hydrogels appears as a consequence of the competition between the increase in J due to* Π_{ion} *and the resistance to preventing J from attaining* J_{ult}.

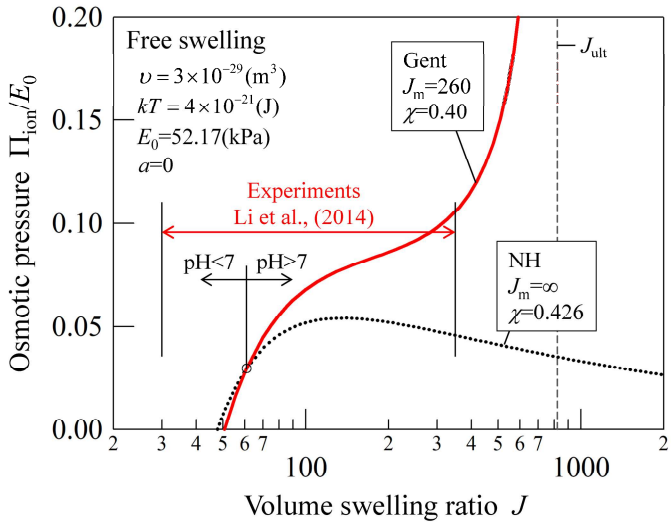

Fig. 11. Relation of J and Π_{ion} for $\chi = 0.40$ with the G model and $\chi = 0.426$ with the NH model. The value of χ was fitted based on the set of $J = 61$ and $\Pi_{ion} = 1550$ (Pa) at pH = 6.5. The NH model predicts that the gel is dissolved when $\Pi_{ion}/E_0 > 0.05$ and cannot reproduce the large increase of J with increasing Π_{ion}. In contrast, the G model successfully reproduces the large increase of J as a process where J approaches J_{ult}.

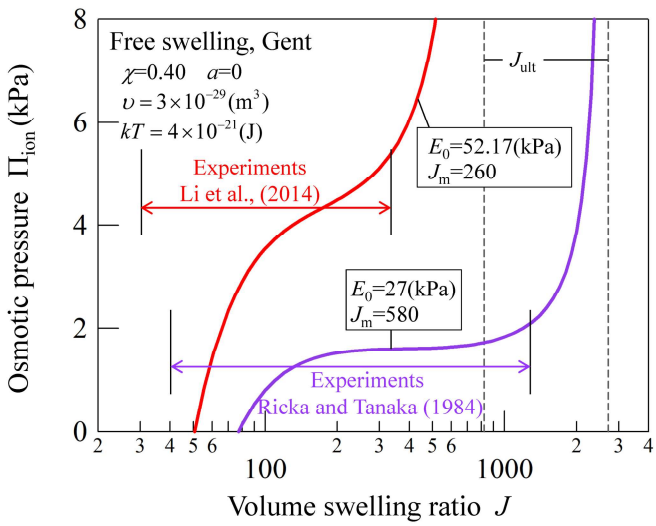

Fig. 12. Comparison of the two different pH sensitive gels by Li et al. [17] and Ricka and Tanaka [38], and the effects of E_0 and J_m. When E_0 is smaller and J_m is larger, the steep increase of J is clearly observed. The different tendency of the two gels in the experiments is comprehensively interpreted via considering the ultimate swelling because of limiting chain extensibility.

Fig. 12 shows a comparison of two different pH sensitive gels. According to Li et al. [17], Tanaka's gel [38] was presumed to have $E_0 = 27$ (kPa) and $J_m = 580$. Both of Li's and Tanaka's gels are assumed to have a common χ value of 0.40 for the G model. Although Fig. 12 shows the considerable difference of the two gels, these predictions are in very good agreement with the experiments (see the figure 5a in Li et al. [17]). In other words, the experiments showed that for Li's gel, the increase of Π_{ion} from 0 to 4000 (Pa) caused the monotonic increase of J from 30 to 350, whereas for Tanaka's gel, the steep increase of J from 90 to 1000 occurred around $\Pi_{ion} = 1300$ (Pa), and subsequently the increase of J needed again the increase of Π_{ion}.

Fig. 12 shows a comprehensive understanding of the different responses of Li's and Tanaka's gels. First, both of the responses display the inverted S shape regardless of the combination of E_0 and J_m. This characteristic shape is formed as a result of the competition between the increase in swelling because of the increase of Π_{ion} and the resistance generated when approaching the ultimate value J_{ult}. In Eq. (30), Π_{ion} is

normalized by E_0, i.e., Π_{ion}/E_0; thus, when E_0 becomes smaller, the effect of Π_{ion}/E_0 becomes relatively larger. Tanaka's gel takes the larger value of J at the same value of Π_{ion}. Further, since Tanaka's gel has the larger value of J_m, $J_{ult} = 2709$ is significantly larger than $J_{ult} = 820$ for Li's gel. The combination of a smaller value of E_0 and a larger value of J_m forms a clear plateau region of Π_{ion} in the inverted S shape. This plateau region is terminated upon approaching J_{ult}. In contrast, the response of Li's gel does not have the plateau region, which is understood by the combination of a relatively large value of E_0 and a relatively small value of J_m.

The comparison of the two different gels shows two fundamental aspects for pH sensitive hydrogels: the dependence of J on Π_{ion} appears through E_0 and J_m, whereas the change of Π_{ion} is caused by the individual concentrations of mobile ions in the external solvent, which is currently quantified using the Donnan theory [17,39]. However, a more quantitative prediction will need further modification of the Flory–Huggins solution theory (e.g., [2,17]) and/or the model of the elastic strain energy (e.g., [18,28,40–44]). The interaction parameter χ may not be a constant but depend on J [2,4,32]. Li et al. [17] experimentally estimated the unified master curve of the osmotic pressure due to mixing for pH sensitive hydrogels, instead of using the Flory–Huggins solution theory. In contrast, Okumura et al. [28] introduced two scaling exponents in the NH model to fit the Flory–Rehner theory to the experimental data of natural rubbers in organic solvents. The Donnan theory may also need further modification for the quantitative comparison between experiments and theoretical predictions [17,38,39].

7. Conclusions

In the present study, ultimate swelling characterized by limiting chain extensibility of swollen elastomers was studied. Limiting chain extensibility was introduced into the Flory–Rehner theory using the AB and G models. The difference between these models was unified by defining the single scalar function Ω (Eq. (12)). The inequality derived from the limit included in Ω allowed ultimate analysis to provide the ultimate value of the volume swelling ratio. The ultimate values depend on the type of external forces and are not exceeded at equilibrium swelling. Under uniaxial loading at equilibrium

swelling, deswelling can occur even in tension. Furthermore, the very large swelling behavior of pH sensitive hydrogels were successfully interpreted as a consequence of the competition between the increase in the osmotic pressure due to mobile ions and the resistance to prevent the volume swelling ratio approaching the ultimate value. The NH model failed to describe even the qualitative response of pH sensitive hydrogels. The effect of limiting chain extensibility plays an essential role in causing the very large swelling behavior of pH sensitive hydrogels. The developed ultimate analysis should provide a more comprehensive understanding of swollen elastomers undergoing finite deformations.

Finally, although the NH model in the Flory–Rehner theory was simply replaced by the AB or G models in the present study, it must be interesting to consider more advanced elastic strain energies (e.g., [18,28,40–44]). According to [43,44], the elastic strain energy W_e needs to include not only the first invariant I_1 but also the second invariant I_2 (see Section 2) to fit well the experimental data in the small-to-moderate strain range. This I_2 energy term is expected to be linearly added in original elastic strain energies [43,44]. In this specific case, the I_2 energy term gives no effect on the ultimate value of swelling investigated in the present study. That is because the scalar function Ω depends on I_1 and is independent of I_2 (Eq. (12)). When Ω is expressed as a combination of I_1 and I_2, the ultimate value of swelling can depend on I_2. The above-mentioned discussions are worthy and needed when more accurate deformation analysis of swollen elastomers is explored in the future. The findings obtained from these researches including the present study will be useful to design the unique mechanical and swelling properties of gels and biomaterials.

Acknowledgements

The authors thank Dr. Jana Wilmers at the University of Wuppertal, Dr. Makoto Uchida at Osaka City University and Mr. Takafumi Mano at Nagoya University for fruitful comments and discussions. The authors also thank the Edanz Group (www.edanzediting. com/ac) for editing a draft of this manuscript. This research was partially supported by the Japan Society for the Promotion of Science (JSPS) under a

Grant-in-Aid for Scientific Research (B) (No.16H04234) and by the US National Science Foundation (CMMI-1463121).

Appendix A.

Fig. A shows the influence of the logarithmic term of $-a \log J$ included in the elastic strain energies on the osmotic pressure under free swelling (Eq. (19)). The AB+P model was used as the representative model with n=10, 100 and ∞. The response for $n = \infty$ is identical to that in the NH model. At a larger swelling ratio $J > 20$, the effect can be negligible regardless of the value of n. The value of a does not affect the ultimate value of J_{ult}. In contrast, at a smaller swelling ratio $J < 20$, the positive and negative values of $a = 2$ and -2 decreases and increases Π, respectively, which results in providing the additional increase and decrease of J under free swelling, respectively. For the NH model, $a = 0$, 1 and 2 were conventionally used [1,2,19]. For the G model, $a = 2$ was just used [17]. In contrast, Bischoff et al. [45] proposed $a \neq 2$ to introduce a logarithmic term in the AB model [4,16] while $a = 2$ was simply used in Chester and Anand [15]. If the value of a is assumed as the parameter fitted to experiments [28,46], the swelling behavior under $J < 20$ can be adjusted and predicted well.

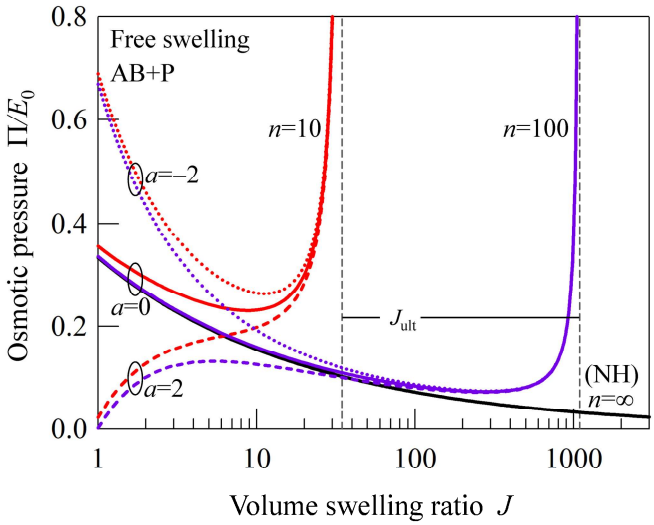

Fig. A. Effect of the logarithmic term $-a \log J$ included in the elastic strain energies on the osmotic pressure under free swelling. The AB+P model was used as the representative model with $n = 10$, 100 and ∞. The response for $n = \infty$ is identical to that in the NH model.

References

[1] Flory, P.J., 1953. Principles of Polymer Chemistry; Cornell University Press: Ithaca, NY.

[2] Treloar, L.R.G., 1975. The Physics of Rubber Elasticity, 3rd ed.; Clarendon Press: Oxford.

[3] Doi, M., 2013. Soft Matter Physics. Oxford University Press: Oxford, UK.

[4] Liu, Z.S., Toh, W., Ng, T.Y., 2015. Advances in mechanics of soft materials: a review of large deformation behavior of hydrogels. Int. J. Appl. Mech. 7, 1530001.

[5] Flory, P.J., Rehner, J., 1943. Statistical mechanics of cross-linked polymer networks II. Swelling. J. Chem. Phys. 11, 521–526.

[6] Hong, W., Liu, Z.S., Suo, Z., 2009. Inhomogeneous swelling of a gel in equilibrium with a solvent and mechanical load. Int. J. Solids Struct. 46, 3282–3289.

[7] Kang, M.K., Huang, R., 2010. A variational approach and finite element implementation for swelling of polymeric hydrogels under geometric constraints. J. Appl. Mech. 77, 061004.

[8] Okumura, D., Kuwayama, T., Ohno, N., 2014. Effect of geometrical imperfections on swelling-induced buckling patterns in gel films with a square lattice of holes. Int. J. Solids Struct. 51, 154–163.

[9] Okumura, D., Inagaki, T., Ohno, N., 2015. Effect of prestrains on swelling-induced buckling patterns in gel films with a square lattice of holes. Int. J. Solids Struct. 58, 288–300.

[10] Boyce, M.C., Arruda, E.M., 2000. Constitutive models of rubber elasticity: a review. Rubber Chem. Technol. 73, 504–523.

[11] Arruda, E.M., Boyce, M.C., 1993. A three-dimensional model for the large stretch behavior of rubber elastic materials. J. Mech. Phys. Solids 41, 389–412.

[12] Gent, A.N., 1996. A new constitutive relation for rubber. Rubber Chem. Technol. 69, 59–61.

[13] Boyce, M.C., 1996. Direct comparison of the Gent and the Arruda–Boyce constitutive models of rubber elasticity. Rubber Chem. Technol. 69, 781–785.

[14] Horgan, C.O., Saccomandi, G., 2002. A molecular-statistical basis for the Gent constitutive model of rubber elasticity. J. Elasticity 68, 167–176.

[15] Chester, S.A., Anand, L., 2010. A coupled theory of fluid permeation and large deformations for elastomeric materials. J. Mech. Phys. Solids 58, 1879–1906.

[16] Chester, S.A., Anand, L., 2011. A thermo-mechanically coupled theory for fluid permeation in elastomeric materials: application to thermally responsive gels. J. Mech. Phys. Solids 59, 1978–2006.

[17] Li, J., Suo, Z., Vlassak, J.J., 2014. A model of ideal elastomeric gels for polyelectrolyte gels. Soft Matter 10, 2582–2590.

[18] Boyce, M.C., Arruda, E.M., 2001. Swelling and mechanical stretching of elastomeric materials. Math. Mech. Solids 6, 641–659.

[19] Terzaghi, K., 1925. Erdbaumechanik auf bodenphysikalischer grundlage; Franz Deuticke, Liepzig-Vienna.

[20] Biot, M.A., 1941. General theory of three-dimensional consolidation. J. Appl. Phys. 12, 155–164.

[21] Truesdell, C., 1962. Mechanical basis of diffusion. J. Chem. Phys. 37, 2336–2344.

[22] Bowen, R.M., 1976. Theory of Mixtures, Part I. In: Eringen, A.C., editor. Continuum Physics 3, 1–127.

[23] Shi, J.J.J., Rajagopal, K.R., Wineman, A.S., 1981. Applications of the theory of interacting continua to the diffusion of a fluid through a non-linear elastic media. Int. J. Eng. Sci. 19, 871–889.

[24] Pence, T.J., 2012. On the formulation of boundary value problems with the incompressible constituents constraint in finite deformation poroelasticity. Math. Meth. Appl. Sci. 35, 1756–1783.

[25] Selvadurai, A.P.S., Suvorov, A.P., 2016. Coupled hydro-mechanical effects in a poro-hyperelastic material. J. Mech. Phys. Solids 91, 311–333.

[26] Bouklas, N., Huang, R., 2012. Swelling kinetics of polymer gels: comparison of linear and nonlinear theories. Soft Matter 8, 8194–8203.

[27] Durning, C.J., Morman, Jr., K.N., 1993. Nonlinear swelling of polymer gels. J. Chem. Phys. 98, 4275–4293.

[28] Okumura, D., Kondo, A., Ohno, N., 2016. Using two scaling exponents to describe the mechanical properties of swollen elastomers. J. Mech. Phys. Solids 90, 61–76.

[29] Jedynak, R., 2015. Approximation of the inverse Langevin function revisited. Rheol. Acta 54, 29–39.

[30] Cohen, A., 1991. A Padé approximant to the inverse Langevin function. Rheol. Acta 30, 270–273.

[31] Cai, S., Suo, Z., 2012. Equations of state for ideal elastomeric gels. Europhysics Letters 97, 34009.

[32] Li, J., Hu, Y., Vlassak, J.J., Suo, Z., 2012. Experimental determination of equations of state for ideal elastomeric gels. Soft Matter 8, 8121–8128.

[33] Hong, W., Zhao, X., Zhou, J., Suo, Z., 2008. A theory of coupled diffusion and large deformation in polymeric gels. J. Mech. Phys. Solids 56, 1779–1793.

[34] Kang, M.K., Huang, R., 2010. Swelling-induced surface instability of confined hydrogel layers on substrates. J. Mech. Phys. Solids 58, 1582–1598.

[35] Wu, Z., Bouklas, N., Huang, R., Swell-induced surface instability of hydrogel layers with material properties varying in thickness direction. Int. J. Solids Struct. 50, 578–587.

[36] Bitoh, Y., Urayama, K., Takigawa, T., Ito, K., 2011. Biaxial strain testing of extremely soft polymer gels. Soft Matter 7, 2632–2638.

[37] Liu, M., Ishida, Y., Ebina, Y., Sasaki, T., Hikima, T., Takata, M., Aida, T., 2015. An anisotropic hydrogel with electrostatic repulsion between cofacially aligned nanosheets. Nature 517, 68–72.

[38] Ricka, J., Tanaka, T., 1984. Swelling of ionic gels: quantitative performance of the Donnan theory. Macromolecules 17, 2916–2921.

[39] Marcombe, R., Cai, S., Hong, W., Zhao, X., Lapusta, Y., Suo, Z., 2010. A theory of constrained swelling of a pH-sensitive hydrogels. Soft Matter 6, 784–793.

[40] Ogden, R.W., 1972. Large deformation isotropic elasticity – On the correlation of theory and experiment for incompressible rubberlike solids. Proc. Royal Soc. London A326, 565–584.

[41] Davidson, J.D., Goulbourne, N.C., 2013. A nonaffine network model for elastomers undergoing finite deformations. J. Mech. Phys. Solids 61, 1784–1797.

[42] Drozdov, A.D., Christiansen, J.deC., 2013. Stress–strain relations for hydrogels under multiaxial deformation. Int. J. Solids Struct. 50, 3570–3585.

[43] Puglisi, G., Saccomandi, G., 2016. Multi-scale modelling of rubber-like materials and soft tissues: an appraisal. Proc. R. Soc. A472, 20160060.

[44] Destrade, M., Saccomandi, G., Sgura, I., 2017. Methodical fitting for mathematical

models of rubber-like materials. Proc. R. Soc. A473, 20160811.

[45] Bischoff, J.E., Arruda, E.M., Grosh, K., 2001. A new constitutive model for the compressibility of elastomers at finite deformations. Rubber Chem. Technol. 74, 541–559.

[46] Okumura, D., Mizutani, M., Tanaka, H., Uchida, M., 2018. Effects of two scaling exponents on biaxial deformation and mass transport of swollen elastomers. Int. J. Mech. Sci. (in press).